AD-A089 676 COLD REGIONS RESEARCH AND ENGINEERING LAB HANOVER NH F/G 20/11
DYNAMIC TESTING OF FREE FIELD STRESS GAGES IN FROZEN SOIL.(U)
JUL 80 G W AITKEN, D G ALBERT, P W RICHMOND
UNCLASSIFIED CRREL-SR-80-30 NL

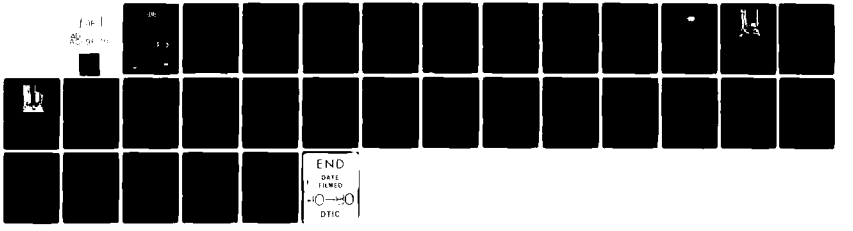

END
DATE FILMED
DTIC

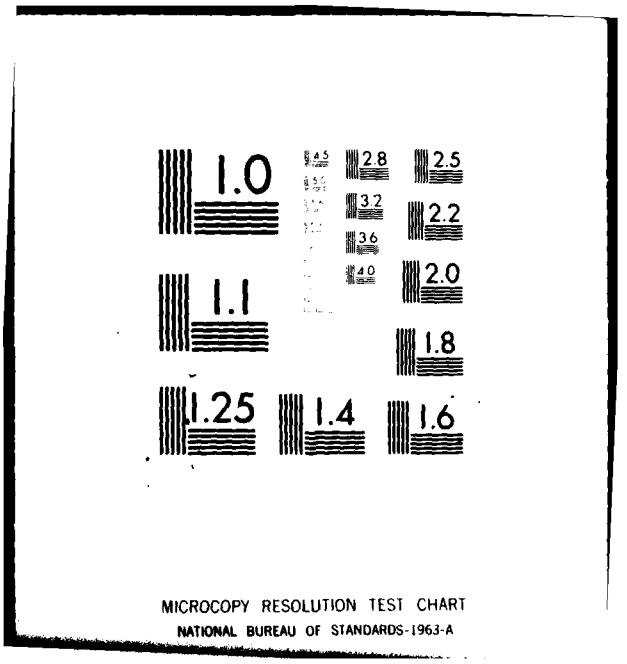
1.0
1.1
1.25
1.4
1.6
1.8
2.0
2.2
2.5
2.8
3.2
3.6
4.0
MICROCOPY RESOLUTION TEST CHART
NATIONAL BUREAU OF STANDARDS-1963-A

JL

Special Report 80-30

July 1980

LEVEL II

12

AD A089676

DYNAMIC TESTING OF FREE FIELD STRESS GAGES IN FROZEN SOIL

G.W. Aitken, D.G. Albert and P.W. Richmond

UNITED STATES ARMY
CORPS OF ENGINEERS
COLD REGIONS RESEARCH AND ENGINEERING LABORATORY
HANOVER, NEW HAMPSHIRE, U.S.A.

Unclassified (17) CRREL-SR-80-30

SECURITY CLASSIFICATION OF THIS PAGE (When Data Entered)

REPORT DOCUMENTATION PAGE

READ INSTRUCTIONS BEFORE COMPLETING FORM

(9)

1. REPORT NUMBER: Special Report 80-30
2. GOVT ACCESSION NO.: AD-A089676
3. RECIPIENT'S CATALOG NUMBER:

(6)

4. TITLE (and Subtitle): DYNAMIC TESTING OF FREE FIELD STRESS GAGES IN FROZEN SOIL
5. TYPE OF REPORT & PERIOD COVERED:
6. PERFORMING ORG. REPORT NUMBER:

(10) Leung

7. AUTHOR(s): C.W. Aitken, D.G. Albert and P.W. Richmond
8. CONTRACT OR GRANT NUMBER(s):

9. PERFORMING ORGANIZATION NAME AND ADDRESS:
U.S. Army Cold Regions Research and Engineering Laboratory
Hanover, New Hampshire 03755

10. PROGRAM ELEMENT, PROJECT, TASK AREA & WORK UNIT NUMBERS:
DA Project
(16) 4A161101A91D

11. CONTROLLING OFFICE NAME AND ADDRESS:
U.S. Army Cold Regions Research and Engineering Laboratory
Hanover, New Hampshire 03755

12. REPORT DATE:
(11) July 1980

13. NUMBER OF PAGES:
32

14. MONITORING AGENCY NAME & ADDRESS (if different from Controlling Office):
(12) 30

15. SECURITY CLASS. (of this report):
Unclassified

15a. DECLASSIFICATION/DOWNGRADING SCHEDULE:

16. DISTRIBUTION STATEMENT (of this Report)

Distribution unlimited; approved for public release.

17. DISTRIBUTION STATEMENT (of the abstract entered in Block 20, if different from Report)

18. SUPPLEMENTARY NOTES

19. KEY WORDS (Continue on reverse side if necessary and identify by block number)

Soil
Soil dynamics
Soil tests
Stresses
Wave propagation

20. ABSTRACT (Continue on reverse side if necessary and identify by block number)

This report describes an attempt to develop a procedure for dynamic calibration of free-field soil stress gages embedded in a soil sample. The method presented utilizes a drop-type impact testing machine and a small, instrumented container of soil. The velocity history of a shock pulse applied to the soil sample is measured and the applied stress computed; this value is then compared with data obtained from stress gages embedded in the soil. The results showed that the procedure is adequate for unfrozen soil, but for frozen soil the accuracy in the measurement of compressional wave velocity needs to

DD FORM 1 JAN 73 1473 EDITION OF 1 NOV 65 IS OBSOLETE

Unclassified

SECURITY CLASSIFICATION OF THIS PAGE (When Data Entered)

20. (cont'd).

be increased to obtain useful results.

PREFACE

This report was prepared by George W. Aitken, Research Civil Engineer and Donald G. Albert, Geophysicist, both of the Geophysical Sciences Branch, Research Division; and Paul W. Richmond, Mechanical Engineer, Civil Engineering Research Branch, Experimental Engineering Division, U.S. Army Cold Regions Research and Engineering Laboratory. This study was funded under the FY 1978 In-House Laboratory Independent Research (ILIR) Program.

The authors express their appreciation to North Smith for his suggestions and help in initiating the test program, to Dennis Farrell for his guidance in preparing the soil samples and assistance in conducting the tests, and to Glenn Durell for his assistance with the instrumentation and static calibration. The report was reviewed for technical content by Dr. William F. St. Lawrence and Dr. Malcolm Mellor.

CONTENTS

ILLUSTRATIONS

TABLES

NOMENCLATURE

A_o = acceleration measured at base of soil sample, m/s^2

σ_i = stress measured by gage placed 1 in. from base of container, Pa

V_c = compressional wave velocity, m/s

τ = duration of acceleration pulse, s

ρ = mass density, kg/m^3

$\dot{Z}$ = particle velocity, m/s

$\dot{Z}_{fs}$ = free surface velocity, m/s

σ_c = stress calculated at sample base, Pa

σ_m = stress measured at sample base, Pa

k = gage registration factor, = σ_m/σ_c

AAB c.d. - TEST IDENTIFICATION

AA - Soil type

MS: Manchester silt, HS: Hanover silt

B - Container type

S: Small container (7.25 in. diam, 6 in. deep)
(0.18 m diam, 0.15 m deep)

L: Large container (7.25 in. diam, 12 in. deep)
(0.18 m diam, 0.31 m deep)

B: Big container (11.5 in. diam, 10 in. deep)
(0.29 m diam, 0.25 m deep)

c - Test sample number

d - Drop number

DYNAMIC TESTING OF FREE FIELD STRESS GAGES IN FROZEN SOIL

George W. Aitken, Donald G. Albert and Paul W. Richmond

INTRODUCTION

The objective of this work was to investigate the feasibility of using a drop-type impact testing machine for dynamic calibration of free field stress gages in frozen soil. Procedures are described for both static and dynamic calibration of dynamic soil stress gages. The static procedure is similar to the factory method and the results obtained are comparable. The dynamic procedure consisted of mounting a small container of soil on a drop-type test machine. The velocity history of the shock pulse applied to the soil was measured and the stress applied to the sample computed. This computed stress was then compared with stress data obtained from gages embedded in the soil. The results showed that this procedure is adequate for unfrozen soil, but it does not appear feasible for frozen soil since the compressional wave velocity resolution was too low.

BACKGROUND

This report investigates the applicability of free field stress gages for making measurements of stress wave attenuation in frozen soils. Similar data are already available for other materials (Fig. 1).

Information is already available on the design of free-field soil stress gages for use in unfrozen soils. Details of the most widely used gage were discussed by Ingram (1968). This gage, the Kulite VM-750 soil stress gage, also known as an SE gage (Fig. 2), is used in the tests discussed here. It has a 2-in. diameter and is 0.266 in. thick (5.08 cm diameter, 0.68 cm thick). The sensing area has a diameter of 0.75 in. (1.9 cm). The gage modulus is 4.52×10^5 psi (3.12 GPa) and its natural frequency is 40 kHz. These gages are manufactured by Kulite Semi-conductor Products, Inc. and are available in 200-psi (1.4-MPa) and 3000-psi (20 MPa) ranges (different diaphragm thicknesses) for about $400 each.

STATIC CALIBRATION

The gages are calibrated at the factory under a static load by placing them in a steel sphere and pressurizing the sphere to the desired level. The factory obtains their published gage sensitivity by using only the gage output obtained at maximum rated pressure, i.e. 200 or 3000 psi. This calibration is presented in terms of voltage output per volt-excitation per psi and ranges from about 0.2 mV/V psi for the 3000-psi gages up to 0.3 mV/V psi for the 200-psi gages.

A slightly different static calibration procedure was utilized at CRREL. The gages were clamped in a press to seat 11/16-in. ID rubber O-rings against the 3/4-in. diameter active gage area. The space inside the O-rings was then pressurized with hydraulic fluid, with equal pressure applied to both sides of the gage. Gages with a 200-psi range were checked to 250 psi (1.7 MPa) and the 3000-psi gages to 4000 psi (28 MPa). The data from these calibration runs are presented in Table 1.

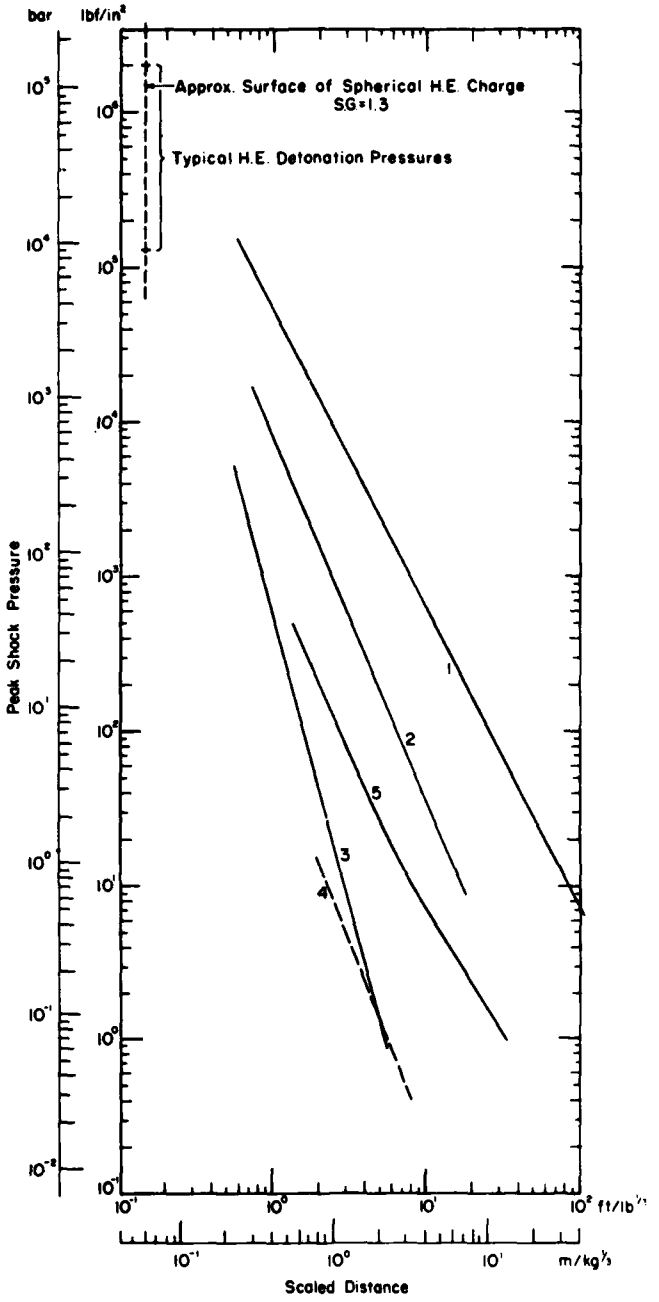

Figure 1. Stress wave attenuation in various materials. 1) Granite, 2) glacier ice, 3) ice cap snow, 4) seasonal snow, 5) air (Mellor 1972). (Note: 1 psi = 6.894kPa, H.E. = high explosive, S.G. = specific gravity).

Table 1. Static calibration data.

Pressure (psi)	Gage serial numbers (200-psi gages) 1570	1572	067	1553	025	1510	1522	094	1616
				CRREL data					
0	1.0mV	1.6mV	2.1mV	-0.5mV	0.2mV	-1.3mV	0.8mV	0.6mV	1.7mV
50	97.4	116.5	114.0	100.7	105.7	97.0	114.3	110.4	105.4
100	195.3	232.9	226.7	206.4	212.2	198.0	227.7	220.0	211.0
150	296.2	343.7	340.5	307.0	317.5	296.9	340.5	328.4	315.0
200	397.0	455.9	453.8	411.8	422.6	397.2	453.0	437.5	420.5
250	499.3	567.7	569.9	514.3	530.4	498.7	568.7	550.9	528.6
Sensitivity[a]	0.198	0.227	0.226	0.206	0.211	0.199	0.226	0.218	0.209

				Kulite data			
0	4.2mV	-11.5mV	0.7mV	-5.3mV	1.0mv	6.0mV	
40	98.4	108.2	99.4	97.4	111.1	104.2	
80	147.2	216.5	198.5	194.2	221.6	208.2	
120	296.0	324.9	297.8	291.2	333.3	312.4	
160	395.2	433.8	397.1	388.1	444.3	416.5	
200	494.8	542.5	496.3	484.9	555.1	520.4	
Sensitivity[a]	0.200	0.226	0.206	0.200	0.227	0.210	
Sensitivity[b]	0.2474	0.2712	0.2481	0.2424	0.2776	0.2602	

CRREL data (3000-psi gages)

	1358	1384	1350
0	4.6mV	2.0mV	1.3mV
500	116.6	121	106.4
1000	230.4	237.7	214.0
1500	348.5	353.8	327.5
2000	466.2	479.5	437.6
2500	587.4	599.7	552.1
3000	711.0	734.4	667.9
4000	954.4	---	909.0
Sensitivity[c]	0.0235	0.0240	0.0223

a Sensitivity obtained from linear regression analysis of 0-200 psi data
b Sensitivity reported by manufacturer using 200-psi data only
c Sensitivity from 0-3000 psi

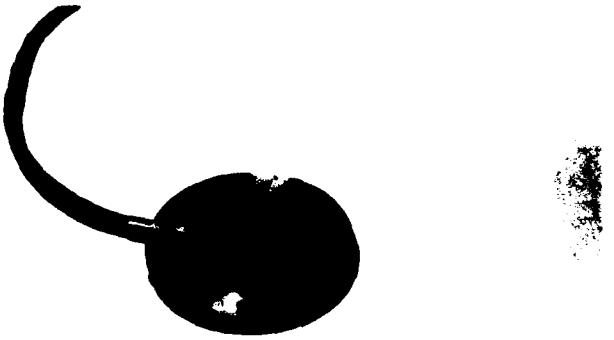

Figure 2. Dynamic SE stress gage.

Gage sensitivity was calculated from these data using a linear least squares fit to the 0-200 and 0-3000 psi data points. The gages exhibited excellent linearity over this range and had no undesirable hysteretic effects. Additionally, the 200-psi gages were found to be linear up to 400 psi (2.8 MPa). The CRREL calibration does not compare well with the single-point sensitivity reported by Kulite but agreement is good if the Kulite data are also analyzed using the least-squares technique. This least-squares sensitivity was selected as being the most representative of gage performance.

The U.S. Army Engineer Waterways Experiment Station (WES) has also compared these two calibration procedures and obtained similar results (Ingram 1968). WES calibrated the gages dynamically (embedded in unfrozen soil) in their *blast-load-generator* facility. They determined that, when placed in unfrozen soil, these gages over-register by factors up to 1.3. WES tried some limited calibration in frozen soil utilizing this technique, but it did not appear to be feasible.

DYNAMIC CALIBRATION

General

A primary reason for the over-registration of the stress gages determined in the dynamic calibration tests conducted by WES was thought to be the difference in modulus between the gages and the unfrozen soil in which they were installed. The elastic modulus of frozen soils, however, is high

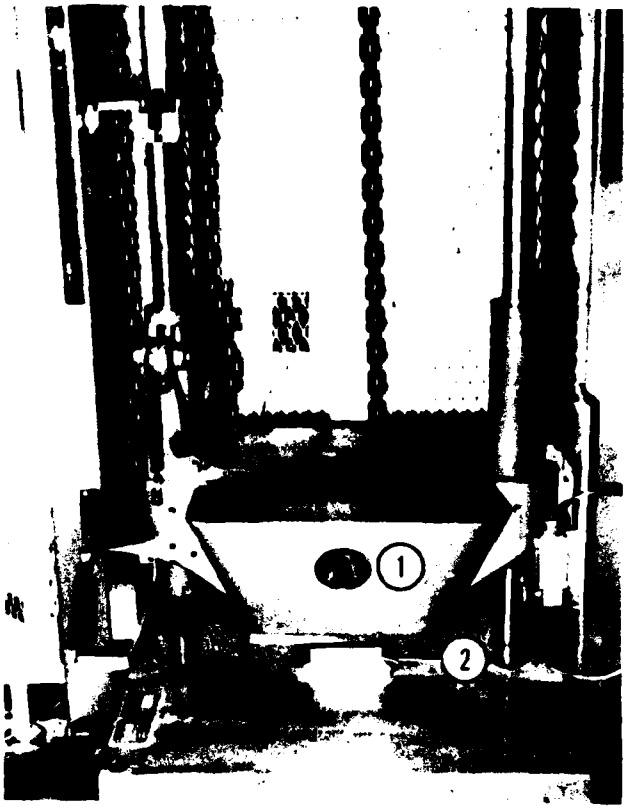

Figure 3. LAB model SD-16-80-200 impact testing machine. (Note: 1. Drop Table, 2. Impact Pad).

enough to be similar to that published for the stress gage itself (4×10^5 psi), so that the gage's performance in frozen soils may be markedly different from its performance in unfrozen soils. The dynamic behavior of the gages in frozen soil was therefore investigated.

It was reasoned that such tests might be accomplished using a drop-type impact testing machine such as the LAB model SD-16-80-200 available at CRREL (Fig. 3). The test procedure envisioned measuring the velocity history of a shock pulse transmitted into a soil sample attached to the drop table of the shock machine. If this measured velocity was assumed to represent the free surface velocity of the soil, the stress at the surface of the sample could then be computed. Stress at the base of the sample could also be determined by extrapolation, using a stress/depth curve defined by stress data from gages installed at three or more depths in the soil. Finally, comparison of the computed and measured stress at the soil surface would provide an indication of the accuracy of the gages.

It was recognized that this might not be a calibration procedure in the strict sense of the word, but it was hoped that any tendency for large, erroneous gage readings, caused by some unanticipated interaction between the gage and frozen soil, could at least be detected.

Table 2. Physical properties of soil test samples.

a. Frozen samples

Test	Date	Temp (°C)	γ_w (lb/ft^3)	WC (%)	Thermocouple 1	2	3	4	5	Note
MSS1.1	12/22/77	-3	121	19						
HSL1.4	3/2/78	-28	119	21	-2.5	-27.9	-31.9	-26.9	--	A
HSL2.1	3/3/78	-27	121	25	-7.0	-22.8	-33.3	-24.7	--	A
HSL3.4	3/24/78	-13	116	19	-6.0	- 3.7	-13.2	- 9.3	--	B
3.5	"	"	"	"	-6.0	- 3.7	-13.2	- 9.3	--	B
3.6	"	"	"	"	-6.0	- 3.7	-13.2	- 9.3	--	B
HSB2.1	8/16/78	-19	122	--	-12.6	-19.8	-19.6	-19.0	-19.8	C
2.2	"	"	"	"	"	"	"	"	"	C
2.3	8/17/78	-20	"	"	-23.5	-29.9	-29.8	-28.8	-29.9	C
2.4	"	"	"	"	"	"	"	"	"	C

b. Unfrozen samples

HSS1.1	2/23/78	+19	121	19
1.2	"	"	"	"
HSS2.1	3/24/78	+19	120	--
2.2	"	"	"	"
HSB4	10/23/79	--	--	--

Note A: Thermocouple locations:

No. 1	Center of base
No. 2	One inch above no. 1
No. 3	Five inches above no. 1
No. 4	Six inches above base on side wall

Note B: Thermocouple locations:

No. 1	Center of base
No. 2	On base near side wall
No. 3	Four inches above No. 1
No. 4	Four inches above No. 2

Note C: Locations unknown.

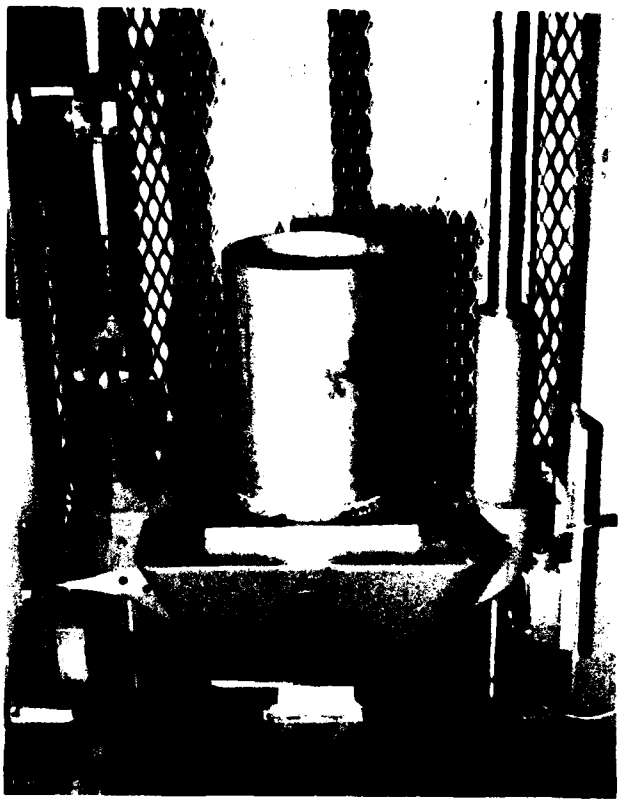

Figure 4. LAB test machine with 12-in.-deep container installed.

Sample Preparation

Samples of Manchester silt and Hanover silt were used for these tests. The physical properties of the samples are given in Table 2. These soils were selected because they were readily available and some data on modulus and wave velocity were also known (Kaplar 1969, Stevens 1975). A moisture content of approximately 20% was selected for ease of compaction. The soil was compacted in 1- or 2-in.-thick layers in cylindrical aluminum sample containers using a 4-lb drop hammer with a 12-in. drop. A gage-sized cavity was excavated in the top of the layer, and a gage installed with soil carefully compacted around it. The surface of the soil was scarified and another layer placed and compacted. Copper-constantan thermocouples were embedded at several locations in the sample (Table 2). After the compaction and gage installation were completed, the soil samples were placed in a cold chamber at a temperature of -30°C so that freezing occurred quickly, and moisture migration in the samples was minimized.

Three different sample containers were used in the tests. The first, container S, was 7 1/4 in. in diameter and 6 in. deep and had 3/8-in.-thick walls. The second, container L, had the same diameter and wall thickness, but was 12 in. deep, while the third, container B, had an 11 1/2-in. diameter

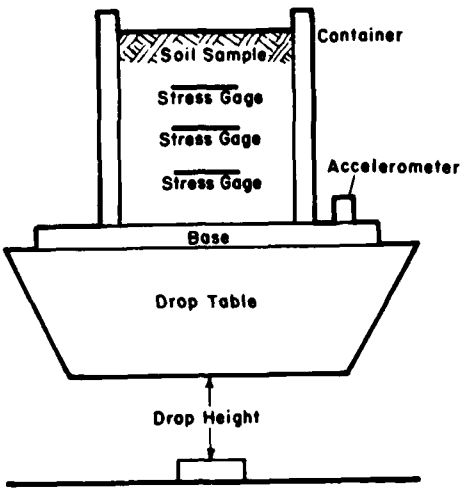

Figure 5. Schematic of soil container.

(the largest diameter that would fit on the shock test machine), and was 10 in. deep with 1/4-in.-thick walls. The 12-in.-deep container installed on the LAB test machine is pictured in Figure 4.

Test Procedure

The frozen soil sample was placed in a temperature chamber at the desired test temperature for about 24 hours prior to testing. The soil container was then bolted onto the drop table and an accelerometer attached to the container base plate (Fig. 5).

The LAB impact test machine was located in an ambient temperature laboratory. Various ways of cooling its shock table, using ice and dry ice, were attempted prior to mounting the frozen samples, but the shock table was never substantially cooled. Therefore, local melting of the sample at its base was possible if any significant time elapsed between placing the sample on the drop table and actually conducting the test. However, the temperature data in Appendix A indicate that melting only occurred during test HSL 3, probably because of long delays to correct an instrumentation problem.

The drop height for the tests was selected so that it would be high enough to produce a reasonable input pulse level but not high enough to cause sample failure. The average drop height was about 12 in.

Instrumentation

Vishay model BA-4 bridge amplifiers (having a bandwidth of 10 kHz) were initially used as signal conditioning amplifiers for the gages. These amplifiers are not designed for the high output levels of the semiconductor type strain gages used in the soil stress gages, so a 10:1 voltage divider was used and the bridge supply voltage was set at only 1 V (instead of the recommended 10). This reduced the input voltage level to the Vishay amplifiers

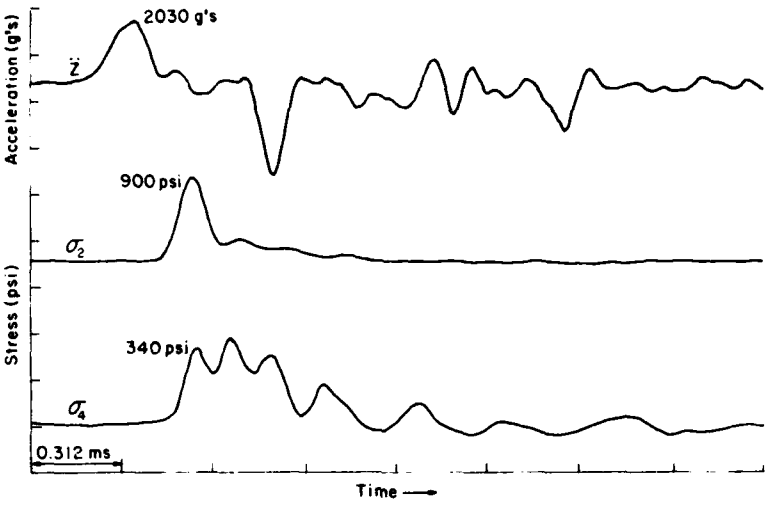

Figure 6. MSS 1.1 Oscillogram.

sufficiently so that when operated at their lowest gain setting (100), output voltage was maintained below the amplifier saturation level of 2.5 V.

These amplifiers were replaced after test HSL 3.6 with Bell and Howell model 1-183 transducer signal conditioners that are specifically designed for the high output levels of semiconductor strain gages. With these amplifiers the recommended 10-V bridge excitation voltage was used and a voltage divider was not required on the output of the gages.

The outputs from the stress gages in the soil sample and the accelerometer used to monitor the input pulse were recorded on analog magnetic tape and subsequently played back on an oscillograph recorder (Fig. 6). The frequency response of this system is linear up to 5 kHz. Temperature data were recorded immediately after each test using a direct reading digital thermometer.

Data Reduction Method

By measuring the compressional wave velocity V_c and mass density ρ of a soil sample, the constrained modulus can be determined from

$$M = V_c^2 \rho \qquad (1)$$

M is related to Young's modulus E by the equation $M = E(1-\nu)/[(1-2\nu)(1+\nu)]$, where ν is Poisson's ratio. Assuming the shock pulse $\ddot{z}(t)$ is in the form of a ½ sine pulse (Fig. 7) gives

$$\ddot{z}(t) = A_o \sin\left(\frac{\pi t}{\tau}\right), \quad 0 < t \leq \tau, \qquad (2)$$

$$= 0, \quad t > \tau,$$

where τ is the duration of the pulse and A_o is the peak amplitude (Rubin 1976). Since the accelerometer is mounted at the free surface of

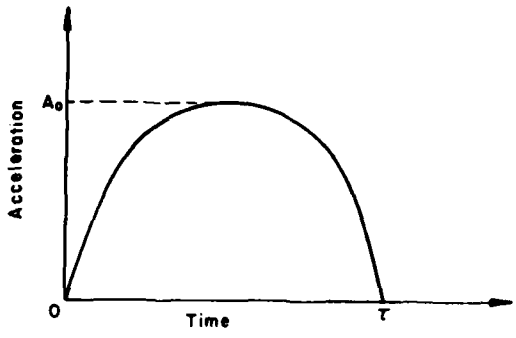

Figure 7. Shock pulse, $\ddot{z}(t)$ (see eq 2).

the container base plate, integrating eq 2 will give the free surface velocity $\dot{z}_{fs}$:

$$\dot{z}_{fs} = \frac{2}{\pi} A_o \tau, \qquad t > \tau \tag{3}$$

while the particle velocity $\dot{z}$ in the aluminum base plate is 1/2 $\dot{z}_{fs}$ (Kolsky 1963, p. 44):

$$\dot{z} = \frac{1}{\pi} A_o \tau, \qquad t > \tau. \tag{4}$$

The stress in a medium is given by the product of the constrained modulus and the ratio of the particle velocity divided by the wave velocity. When the wave passes into the soil sample, its amplitude will be multiplied by a transmission coefficient T of

$$T = \frac{2 V_{al} \rho_{al}}{V_c \rho + V_{al} \rho_{al}} \tag{5}$$

so that the stress in the soil sample can be found from

$$\sigma_c = \frac{\dot{z}}{V_c} M T$$

$$= \frac{1}{\pi} A_o \tau V_c \rho T. \tag{6}$$

With the wave velocity and density of the aluminum base plate, V_{al} and ρ_{al}, known, T and the calculated stress σ_c can be found and compared to the value obtained from the stress gages in the sample to obtain the gage registration factor,

$$K = \frac{\sigma_m}{\sigma_c}. \tag{7}$$

DISCUSSION OF TEST RESULTS

General

The record of test MSS 1.1 (Fig. 6) will be used as an example of the testing method. This test was conducted using Manchester silt soil in the small (7.25-in.-diameter, 6-in.-high) cylinder. The sensors used were an accelerometer at the base of the cylinder (channel 1 on the record), a 3000-psi stress gage 2 in. from the base of the sample (channel 2), and a 200-psi stress gage 4 in. from the bottom. The soil temperature and moisture content were -3°C and 19%, respectively. The soil was wet when this sample was molded and when it was taken apart after the test, a tilting of the gage at the 2-in. depth was discovered.

The data obtained from the oscillogram (Fig. 6) for this test are:

$\ddot{z}_o$ = 2030 g (1.99×10^4 m/s^2, peak acceleration at base of sample)

σ_2 = 900 psi (6.21 MPa, peak stress at 2-in. depth)

σ_4 = 340 psi (2.34 MPa, peak stress at 4-in. depth)

v = 5560 ft/s (1690 m/s^2, velocity between 2- and 4-in. depths)

$\tau = 2.7 \times 10^{-4}$ s (duration of the acceleration pulse).

By assuming logarithmic damping, the stress value from the 2-in. and 4-in. depth gages can be extrapolated to obtain a value of 2380 psi (16.4 MPa) for the stress at the sample base. The stress data are plotted in the top portion of Figure 8, while the travel time data used to find the wave velocity are shown in the bottom. There is a large discrepancy between the apparent velocity of the wave between 0 and 2 in. and 2 and 4 in. This velocity difference was at first attributed to poor coupling between the base of the container and the soil sample.

The velocity used for calculating the free surface velocity and the stress at the sample base was obtained from the slope of the distance versus time curve between the 2-in. and 4-in. locations. Substituting the above values into eq 3 and 6 we find that

$\dot{z}_{fs}$ = 11.2 ft/s (3.41 m/s)

σ_c = 1370 psi (9.45 MPa).

The acceleration data for this test were digitized and integrated to check the validity of the 1/2 sine pulse approximation. This technique gave a free surface velocity of 10.0 ft/s so the approximation appears to be valid.

The large difference between the measured (2380 psi) and calculated (1370 psi) stress values was not anticipated. The sample was dropped a second time (test MSS 1.2) with similar results so it was allowed to thaw, and the gages were removed. At this time a significant tilt in the 2-in.

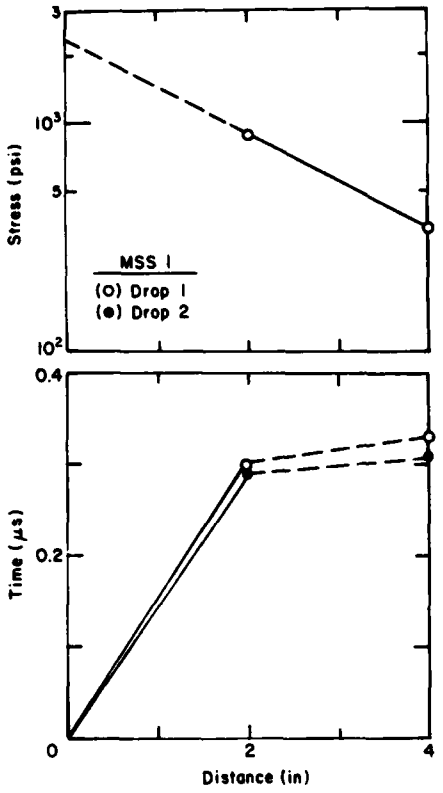

Figure 8. Test MSS 1: top, distance vs log stress; bottom, distance vs travel time.

gage was discovered (about 40 degrees), making the stress and time measurements from this gage questionable. The test results, however, are in agreement with the results of later tests.

The setup of MSS 1 was difficult because the instrumentation checkout was rushed to ensure that the sample would not start to thaw prior to testing. Therefore, to remove any time pressure during test setup and ensure that there were no instrumentation errors affecting the test results, unfrozen samples were tested as well.

The detailed results of additional tests on both frozen and unfrozen samples are presented in Appendix A. Graphs of distance versus measured stress and distance versus travel time are also presented.

Velocity Measurements

A number of problems were encountered during the testing process. Some were temporary and can be attributed directly to problems in operating the equipment (i.e. keeping amplifiers and gages balanced and working properly, etc.), but other problems were more persistent. One major problem with the experimental results was explaining the previously noted velocity discontinuity in the soil sample.

The travel time graphs (bottom of Fig. 8, for example) indicated that the stress wave was apparently traveling at a low velocity until it reached

the first gage, after which it speeded up and traveled past the other gages at a higher velocity. There was no reasonable physical explanation for this behavior since the sample was uniform and the trend of the data points was constrained to pass through the origin (since the wave starts its travel through the sample at the moment of impact).

Theoretical calculations showed that the longer than expected travel time between the accelerometer and the first gage could not be explained by:

1. An air space (or less compacted soil) at the bottom of the container having a low velocity

2. A wave starting at the accelerometer and traveling along the bottom of the cylinder before entering the soil (due to the accelerometer side of the container impacting first)

3. Uncertainty in the measured location of the gages

4. Refraction effects in the container (Appendix B).

Since the theoretical calculations were unable to explain the observed results, some additional tests were conducted, specifically designed to address the apparent velocity discontinuity.

First, a stress gage was placed directly on the bottom of the container beneath the soil. A typical oscillogram and distance versus travel time graph are shown in Figures 9 and 10. The graph indicates that there is a time delay between the response of the stress gages and the accelerometer. This time delay is the cause of the apparent velocity discontinuity. Additional tests with a number of stress gages and accelerometers adjacent to each other on the base plate of the container revealed that the time delay was 0.2 ± 0.05 ms and was not sensor-dependent.

In order to increase the resolution of the time measurements, a four-channel Biomation Model 1015 waveform recorder was used to record the response of the gages with a sampling interval of 0.01 ms. The reading accuracy of records produced using this equipment was found to be 0.01 ms. The records showed a 0.23-ms delay between the piezoelectric accelerometer and the first gage. A time difference of 0.11 ms was also found between a piezoelectric and a piezoresistive accelerometer.

An examination of the oscillograms revealed a possible explanation for the time delay. Figure 11 shows the output of a piezoelectric accelerometer. A small pulse, which is on the order of 100 g and corresponds to a stress of a few psi, precedes a larger one. The stress gage with amplifier gains set for a large stress would not sense this small pulse, but would respond only to the stress produced by the larger impulse. It was thought that the cause of this small pulse was unevenness of the drop table base. The duration t of the small pulse is 0.13 ms, and with a free fall height h of 4 in. results in a sample motion of:

$$x = vt \qquad (8)$$

$$= \sqrt{2gh}\ t$$

$$= \sqrt{(2)(32.2\ \text{ft/s}^2)(12\ \text{in./ft})(4\ \text{in.})}\ \ (1.3 \times 10^{-4}\ \text{s})$$

$$= 0.0072\ \text{in.}\ (0.18\ \text{mm}).$$

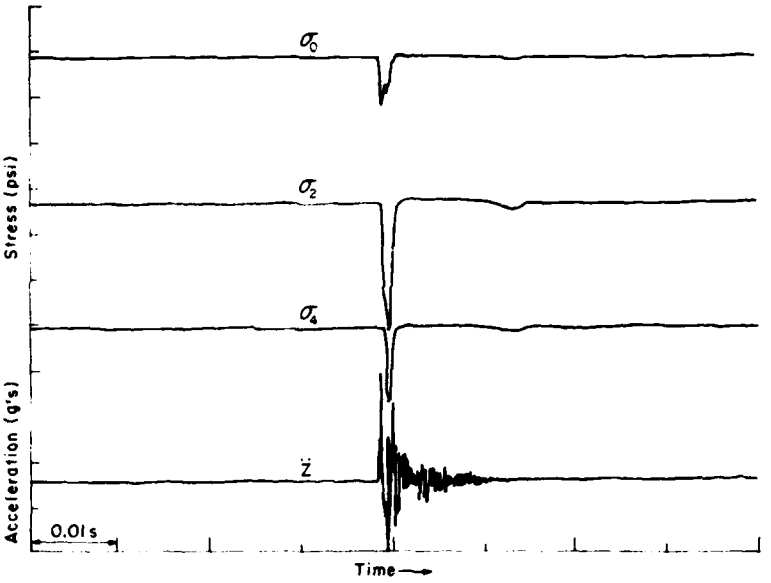

Figure 9. Typical Oscillogram, test HSB 3.4.

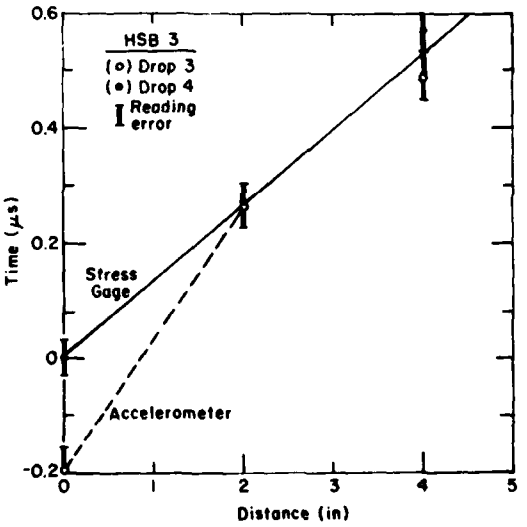

Figure 10. HSB 3.4, distance vs time graph.

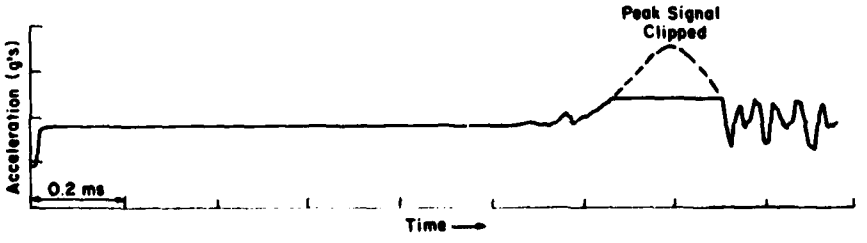

Figure 11. Accelerometer output.

This calculation shows that a slight unevenness or tilt in the drop table can cause the small pulse. This unevenness of the drop table base, when coupled with differences in resolution of the sensors, most likely causes the observed time delay. The time delay between the two pulses decreased as the drop height increased, consistent with the above interpretation.

The accuracy of the present experiment depends directly on the ability to accurately determine the velocity of the stress wave in the soil sample (see eq 5). The velocity measurements themselves are presently limited by the error in determining the travel times. Since

$$v = \frac{x}{t} \tag{9}$$

we can differentiate to obtain

$$\begin{aligned} dv &= \frac{1}{t}\, dx - \frac{x}{t^2}\, dt \\ &= \frac{1}{t}\, dx - \frac{v}{t}\, dt. \end{aligned} \tag{10}$$

Dividing both sides of eq 10 by v gives

$$\frac{dv}{v} = \frac{dx}{x} - \frac{dt}{t}\,. \tag{11}$$

Equation 11 indicates that the percent error in velocity is the sum of the percent errors in the gage placement and time measurements. (The minus sign in the equation indicates that a time value which is too high will decrease the velocity from its true value.) Since the gage placement error during the sample preparation was estimated to be less than 1/4 in., for a gage at a depth of 6 in., the percent error in its location is

$$100 \times \frac{dx}{x} = 100 \times \frac{0.25}{6} = 4.2\%.$$

If we use a nominal, unfrozen soil compressional-wave velocity of 725 ft/s, the travel time to a gage at a depth of 6 in. will be 0.69 ms. An oscillogram reading error of 0.025 ms corresponds to a percent error of

$$100 \times \frac{dt}{t} = 100 \times \frac{0.025}{0.69} = 3.6\%.$$

For frozen soils, however, where the velocity is on the order of 10,000 ft/s (Kaplar 1969, Stevens 1975), the percent error will be much higher. A travel time of 0.05 ms is expected at this velocity, so the same oscillogram reading error as above gives

$$100 \times \frac{dt}{t} = 100 \times \frac{0.025}{0.05} = 50\%.$$

The wide range of velocity values listed in Table A2 is probably due to this reading error. Even with the uncertainty of the time measurements improved to 0.01 ms, the theoretical error is still 20%. To lower the error to 5%, the total travel time measured would have to be increased to 0.2 ms. Thus the travel time of a wave passing through a soil sample at least 2 ft thick (and preferably thicker) would have to be measured. The diameter of the cylindrical containers would also have to be increased to avoid problems with refracted wave arrivals at the deeper sensors. Alternatively, to obtain similar accuracy with the present sample size, the timing resolution would have to be increased to 2.5 μs.

Amplitude Measurements

The amplitudes of the records appear to be consistent. The waveforms detected by each sensor on successive drops were found to be highly repeatable. Problems with the experimental procedures, however, precluded any detailed analysis of the amplitudes of the stress waves. One major problem was difficulty in detecting a stress wave with the deeper gages. This problem was caused by low stress wave amplitude and can be overcome by increasing the amplifier gain settings and increasing the drop height. Other errors were caused by lack of familiarity with this test procedure, resulting in calibration signals that at times were too large, causing the signals to be clipped and making the data unusable. These problems should be easily overcome during future tests.

CONCLUSIONS

1. A drop-type impact test machine can be used to determine stress wave attenuation and compressional wave velocity in unfrozen soils with the test procedures discussed here.

2. The accuracy of this calibration technique is presently limited by the ability to accurately determine compressional wave velocity. To obtain acceptable error bounds with frozen soil samples, the dimensions of the sample need to be increased by a factor of at least two.

3. The observed time delay of 0.23 ± 0.01 ms between the accelerometer and stress gages is most likely due to the unevenness of the drop table base, coupled with differences in resolution of the sensors.

RECOMMENDATIONS

The accuracy of the test procedure must be increased to calibrate the stress gages for frozen soil. This can be accomplished by increasing the size of the sample or by improving the timing instrumentation. If one wishes to use the same drop table in the experiments, the sample size cannot be increased significantly, but the timing accuracy can be improved by adding a multi-channel, high-speed, analog-to-digital converter to the system. The accuracy of the gage calibration factors can also be increased by placing the accelerometer in the soil sample, thus avoiding the use of transmission coefficients in the stress calculations. With these improvements, the testing procedure should be capable of calibrating the stress gages in frozen soils.

LITERATURE CITED

Ingram, J.K. (1968) Development of free field soil stress gage for static and dynamic measurements. U.S. Army Waterways Experiment Station Technical Report 1-814.

Kaplar, C.W. (1969) Laboratory determination of dynamic moduli of frozen soils and ice. U.S. Army Cold Regions Research and Engineering Laboratory Research Report 163.

Kolsky, H. (1963) Stress waves in solids. N.Y. Dover.

Mellor, M. (1972) Controlled release of avalanches by explosives. Advances in North American Avalanche Technology, Symposium. Reno, Nevada, p. 37-49.

Rubin, S. (1976) Concepts in shock data analysis. In Shock and Vibration Handbook, (C.M. Harris and C.E. Crede, Eds.), N.Y.: McGraw-Hill.

Stevens, H.W. (1975) The response of frozen soils to vibratory loads. CRREL Technical Report 265.

APPENDIX A: RESULTS OF TEST DROPS ON FROZEN AND UNFROZEN SOIL SAMPLES

This appendix contains the data, results, and discussion of a number of tests on frozen and unfrozen soil samples. As pointed out in the body of the report, a number of problems were encountered during the tests. The method was eventually determined to be unsatisfactory for accurately calibrating the soil stress gages until the changes mentioned in the conclusions are made. Therefore, the results presented should not be taken as accurate values. These data and results have been included in this report so that future investigators will be aware of the problems encountered in this study.

After MSS 1, described in the main body of the report, the next test was HSS 1. The same sample container was used as in the previous test, but the soil was unfrozen. The results of these test drops are shown in Table A1 and Figures A1a and A1b. These tests again showed the velocity discontinuity at the base of the sample, and the gage over-registration factor, which varied from 0.6 to 2.4.

Another attempt, HSL 1, was made using frozen soil, this time in a larger cylinder (12 in. high) with gages at 2-, 4-, 6- and 8-in. depths in an attempt to better define the stress attenuation curve. The sample temperature was lowered to -28°C to give more time before sample thawing. No data were obtained from drops 1-3 with this sample because of instrumentation problems. HSL 1.4 was the first drop which provided data (see Fig. A2), but no data were obtained from the 200-psi gages installed at 6 and 8 in. The calculated and measured stresses at the sample base were 735 and 1040 psi, respectively, giving an over-registration factor of 1.4. Because this was the fourth drop for this sample, and because no data were obtained from the gages at 6 and 8 in., it was decided to repeat the test using different gages.

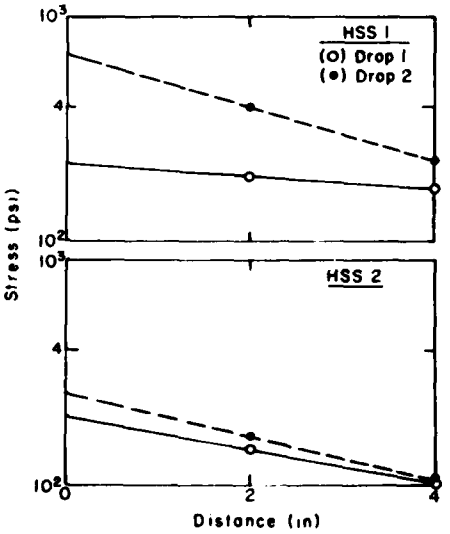

a. Log-stress vs distance (top, test HSS 1; bottom, test HSS 2).

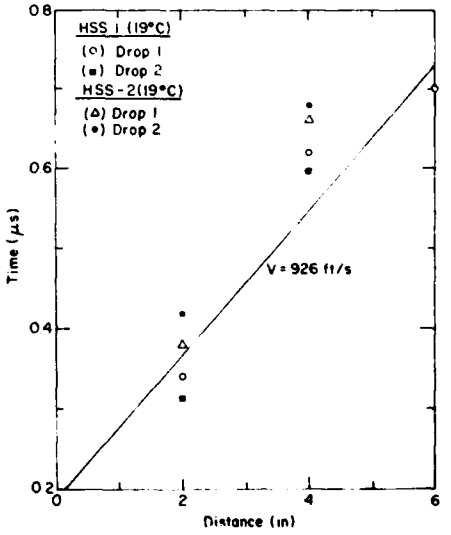

b. Travel time vs distance for unfrozen Hanover silt (test HSS 1 and HSS 2).

Figure A1. Tests HSS 1 and 2.

Table A1. Test data.

Test	Date	Notes	A_o (g)	τ (ms)	σ_1 (psi)	σ_2 (psi)	σ_3 (psi)	t_1 (ms)	t_2 (ms)	t_3 (ms)	t_4 (ms)	V_c (ft/s)	$\dot{Z}$ (ft/s)	σ_c (psi)	σ_m (psi)	K
Frozen samples																
MSS1.1	12/22/77	A,D	2030	0.27	900	340		0.30	0.33			5560	11.2	1370	2380	1.74
MSS1.2								0.29	0.31							
HSL1.4	3/2/78	F	2000	0.29	420	170		0.13	0.19	0.32		2620	11.9	735	1040	1.41
HSL2.1	3/3/78	E	1890	0.17	390	140		0.13	0.19		0.76	2780	6.6	436	1090	2.50
HSL3.4	3/24/78	B,G	1500	0.35	410	270		0.68	0.73			3300	10.7	809	620	0.77
HSL3.5	3/24/78	B,G	1500	0.35	560	430		0.69	0.79			1670	10.7	426	730	1.71
HSL3.6	3/24/78	C,G	1500	0.35	610	520	20	0.48	0.61	0.67	0.82	1540	10.1	395	720	1.82
HSB2.1	8/16/78	E	2050	0.27	310	110	10	0.23	0.24	0.31		4170	11.3	1089	870	0.80
HSB2.2	8/16/78	E	1920	0.29	470	160	30	0.28	0.29	0.35		4760	10.6	1229	1380	1.12
HSB2.3	8/17/78	E	3250	0.17	470	140	60	0.11	0.14	0.20		3700	11.3	1114	1570	1.41
HSB2.4	8/17/78	E	3070	0.22	590	150	70	0.18	0.20	0.29		3030	13.8	1000	2320	2.28
Unfrozen samples																
HSS1.1	2/23/78	E	2870	0.28	200	180		0.34	0.62	0.70		926	16.5	388	220	0.57
HSS1.2	2/23/78	E	2820	0.31	400	230		0.33	0.59			641	17.9	293	700	2.39
HSS2.1	3/24/78	E	1560	0.35	140	100		0.38	0.66			595	11.2	170	200	1.18
HSS2.2	3/24/78	E	1500	0.35	160	110		0.42	0.68			641	10.7	174	230	1.32
HSS4		H	See TABLE A2													

NOTES:

- A: Two-inch gage tilted
- B: Stress measured at 1 in. and 3 in.
- C: Stress measured at 1, 3 and 5 in.; 5-in. stress data not included in calculations
- D: Gages at 2 in. and 4 in.
- E: Gages at 2, 4 and 6 in.
- F: Gages at 2, 4, 6 and 8 in.
- G: Gages at 1, 3, 5 and 7 in.
- H: Gages at 0, 2, 4 and 6 in.

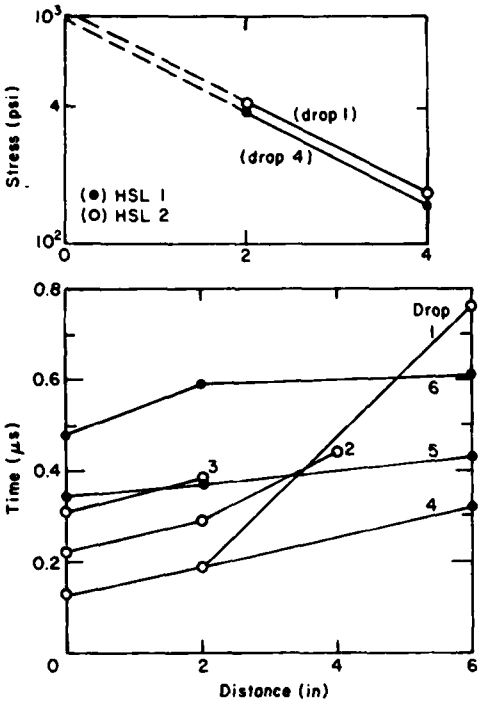

Figure A2. Tests HSL 1.4 and 2.1. Top, log-stress vs distance; bottom, travel time vs distance.

HSL 2 was a repeat of HSL 1. The sample was at a temperature of -27°C and gages were placed at 2, 4, 6 and 8 in. The results of the first drop, HSL 2.1, were almost identical with those from HSL 1.4 (see Fig. A2). The over-registration factor was 2.5, and again no data were obtained from the gages farthest from the sample bottom.

The lack of data from the 6- and 8-in. gages in the previous tests led to the conjecture that a problem might have developed with the 200-psi stress gages. To check this hypothesis, test HSS 2 was conducted using two of these gages in unfrozen soil in the small (6 in. high) container. In this test both gages gave satisfactory signals. The over-registration factors were 1.2 and 1.3, and the travel time data were in agreement with HSS 1 (see Fig. Ala).

For the next test, gages were placed at depths of 1, 3, 5, 7 and 9 in. to ensure that the stress versus depth curve could be well defined. Unfortunately, no acceleration data were obtained for the first three drops on HSL 3, and stress gage data were obtained only from the gages at 1 and 3 in. The problem with the accelerometer was finally rectified for HSL 3.4, but there were still no stress data beyond the 3-in. depth. HSL 3.5 gave similar results, and, finally, after monumental amplifier gain increases, stress gage data were obtained up to the 7-in. depth for HSL 3.6. Figure A3 shows the data for these tests. The velocity discontinuity at the base of the sample is similar to that observed in the previous tests.

At this point it was obvious that some factor other than gages or signal conditioning was causing the problem of missing stress data at the other locations, so an analysis was made of the wave propagation mechanism

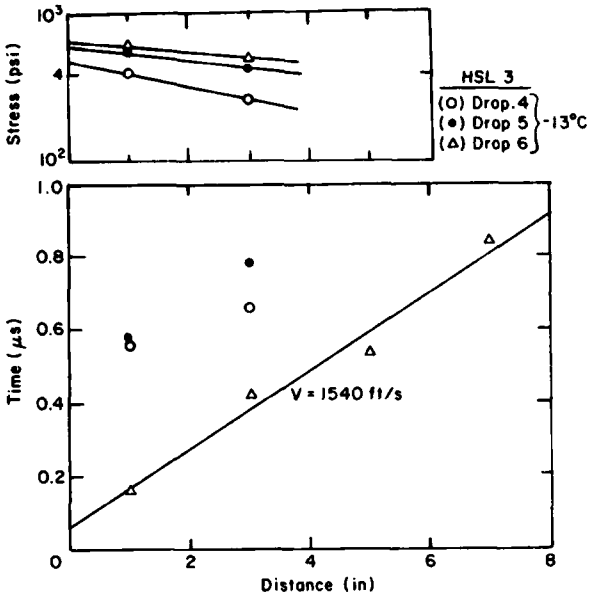

Figure A3. Test HSL 3. Top, log-stress vs distance; bottom, time vs distance.

in the sample container. The analysis (App. B) revealed that in the 7.25-in.-diameter container, a refraction wave will arrive at the same time as the direct stress wave at a gage depth of 7 in. (assuming a frozen soil wave velocity of 10,000 ft/s or 3050 m/s). This calculation indicates a possible problem in measuring the wave velocity in the soil, but does not explain the failure to detect a stress wave at all. Reexamination of the test records showed that the most likely cause of this failure was that the signal level was too low to be detected.

A bigger container was constructed to reduce the effect of the container edges on the experiment as much as possible. The largest container (11.5 in. diameter) that could be used on the drop table was constructed.

In the first test with the 11.5-in.-diameter container (HSB 1.1), gages were placed 1, 2, 3 and 5 in. from the base of the container. At first glance, the data looked good and the sample was dropped again (HSB 1.2). However, analysis disclosed that some instrumentation problem existed and the data were not consistent (i.e. the stress was less at the 1-in. gage than at the 2-in. gage). It was also noted that at the 5-in. gage a very low magnitude (10 psi) reading was obtained, suggesting that a higher input pulse was required. Subsequent drops were done from greater heights in order to obtain data at gages beyond the 5-in. depth.

With all instrumentation problems resolved test HSB 2 was conducted, with gages placed at 2, 4 and 6 in. The sample temperature was -20°C for tests 2.1 and 2.2, and -30°C for tests 2.3 and 2.4. The drop height was doubled for these last two tests. The data are plotted in Figure A4. The velocity discontinuity still existed during the first 2 in. of wave travel in the sample. The results of these four drops produced gage over-registration factors of 0.8, 1.1, 1.4 and 2.3, again all much higher than expected.

At this time a closer investigation of the velocity discontinuity problem was conducted. The procedure and results are described in the main

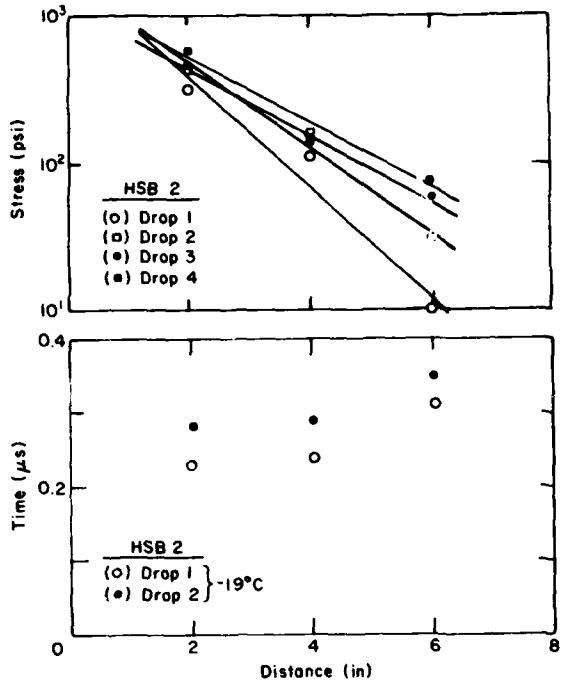

Figure A4. Test HSB 2. Top, log-stress vs distance; bottom, time vs distance.

Table A2. Distance versus travel time data for test HSB 4.

Channel	Depth (in.)	Sensor type[1]	Time (ms)						
Tape record numbers			45-1	45-3	46-1	46-2	46-3	47-2	47-3
1	0	p-r	--	--	--	--	--	-.08	-.07
2	0	s	0	0	0	0	0	0	0
3	2	s	.25	.25	.24	.23	.24	.25	.27
4	4	s	.43	.44	.43	.42	.42	.47	.45
5	6	s	.71	.72	.70	.71	.71	.75	.74
6	0	p-e	-.22	-.21	-.19	-.20	-.19	-.18	-.17

Note 1: p-r = piezoresistive accelerometer
p-e = piezoelectric accelerometer
s = soil stress gage

Note 2: Least squares curve fit of a line through all of the data points gives a velocity of 709 ft/s (216 m/s).

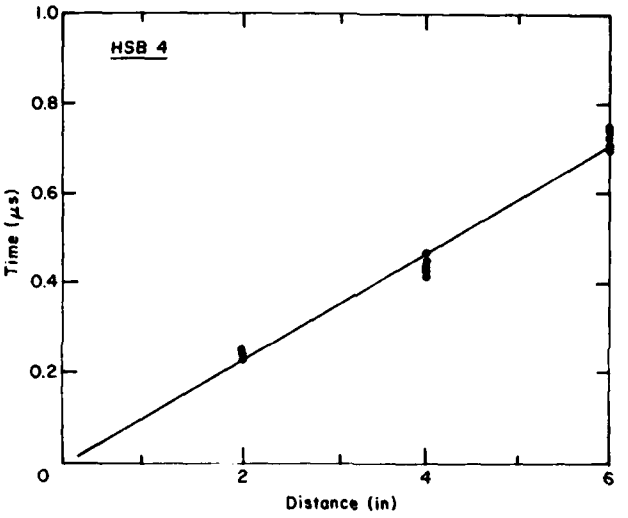

Figure A5. Test HSB 4. Distance vs travel time.

portion of this report. With a stress gage on the base plate at the bottom of the sample, the experiment was repeated, and satisfactory velocity measurements were finally obtained for unfrozen soil.

Table A2 shows the distance versus travel time data, which are plotted in Figure A5. The three drops all agree within the limits of the reading error. The velocity of stress waves through this soil sample is 709 ft/s $\pm$ 28 ft/s (216 m/s $\pm$ 9 m/s). The amplitude data were unusable because an error was made in the calibration procedure. The calibration pulses used were too large, causing the galvanometers to hit their stops, making the calibrated deflection measurements unreliable.

APPENDIX B: REFRACTION EFFECTS IN THE CYLINDER

The experimental geometry and symbols are shown in Figure B1. The travel time for the direct wave to reach the sensor is

$$t_d = \frac{d}{v_1}$$

and the travel time for the refracted wave is

$$t_r = \frac{d-h}{v_2} + \frac{b}{v_1}$$

Snell's law gives $\theta = \text{arc sin } \frac{v_1}{v_2}$ and since

$$b = \frac{r}{\cos\theta} = \frac{rv_2}{v_2^2 - v_1^2}$$

$$h = r \tan\theta = \frac{rv_1}{v_2^2 - v_1^2}$$

the travel time for the refracted wave can be determined. The direct and refracted waves will reach the sensor at the same time when

$$t_d = t_r$$

$$\frac{d}{v_1} = \frac{d-h}{v_2} + \frac{b}{v_1}$$

Multiplying both sides of the above equation gives

$$dv_2 = dv_1 - hv_1 + bv_2$$

and, solving for d,

$$d = \frac{1}{v_2 - v_1}(bv_2 - hv_1)$$

$$= \frac{r}{v_2 - v_1} \quad v_2^2 - v_1^2$$

$$= 4 \quad \frac{v_2 + v_1}{v_2 - v_1}$$

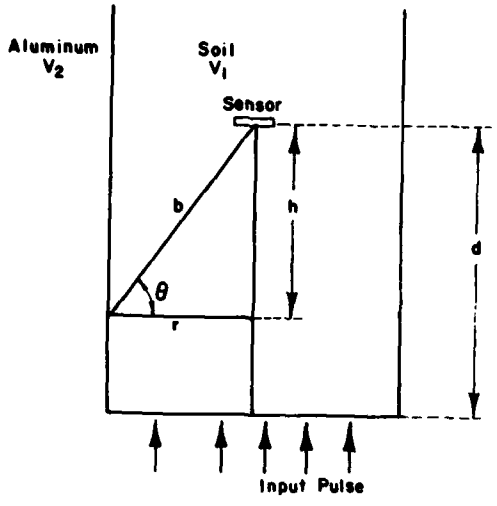

Figure B1. Geometry of sample container.

For unfrozen soil, and assuming that v_1 = 725 ft/s and v_2 = 10,700 ft/s (aluminum),

$$d = 1.044\ r$$

while for frozen soil, assuming v_1 = 10,000 ft/s gives

$$d = 1.964\ r.$$

Two types of cylindrical containers were used in the experiment, one with a diameter of 7.25 in. and the other with a diameter of 11.5 in.; thus the refracted wave will arrive at the same time as the direct wave at a sensor depth of:

	Unfrozen soil	Frozen soil
r (in.)	d (in.)	d (in.)
7.25/2	4	7
11.5/2	6	11